Histol Histopathol (2018) 33: 1311-1321

http://www.hh.um.es

Histology and Histopathology

From Cell Biology to Tissue Engineering

Altered myelination in the Niemann-Pick type C1 mutant mouse

Liang Qiao[1,2], Enhui Yang[1,2], Jiankai Luo[3,4], Juntang Lin[1,2] and Xin Yan[1,2]

[1]Stem Cell and Biotherapy Engineering Research Center of Henan, College of Life Science and Technology, [2]Henan Key Laboratory of Medical Tissue Regeneration, Xinxiang Medical University, Xinxiang, China, [3]Albrecht-Kossel-Institute for Neuroregeneration and [4]Centre for Transdisciplinary Neuroscience Rostock, School of Medicine University of Rostock, Rostock, Germany

Summary. Niemann–Pick type C1 (NPC1) disease is a lysosomal storage disorder caused by mutation of *Npc1* or *Npc2* gene, resulting in various progressive pathological features. Myelin defection is a major pathological problem in Npc1 mutant mice; however, impairment of myelin proteins in the developing brain is still incompletely understood. In this study, we showed that the expression of myelin genes and proteins is strongly inhibited from postnatal day 35 onwards including reduced myelin basic protein (MBP) expression in the brain. Furthermore, myelination characterized by MBP immunohistochemistry was strongly perturbed in the forebrain, moderately in the midbrain and cerebellum, and slightly in the hindbrain. Our results demonstrate that mutation of the *Npc1* gene is sufficient to cause severe and progressive defects in myelination in the mouse brain.

Key words: NPC1, Myelination, Myelin basic protein, Protein expression

Introduction

Niemann-Pick disease type C (NPC) is a fatal autosomal recessive lipid storage disorder characterized by a defect of intracellular lipid metabolism. Mutations in two independent genes of *Npc1* (95% cases in patients) or *Npc2* (5%) cause clinical and biochemical NPC phenotypes. Npc1 is a multi-transmembrane protein distributed in the membrane of late-endosomes/lysosomes (LE/LY) and transports unesterified cholesterol from the LE/LY to the cellular membrane and other intracellular organelles (Subramanian and Balch, 2008). Typically, deficiency of Npc1 protein causes progressive neurological impairment, including reactive gliosis, dysmyelination, and neuronal degeneration, in the central nervous system (CNS) (Pressey et al., 2012; Yu and Lieberman, 2013; Yan et al., 2014).

Npc1 mutant mice ($Npc1^{-/-}$; Loftus et al., 1997) recapitulate many pathological and neurological features of NPC1 patients, and have been widely used as an animal model for investigation of NPC1 disease. The

Offprint requests to: Prof. Dr. Juntang Lin and Dr. Xin Yan, Stem Cell and Biotherapy Engineering Research Center of Henan, College of Life Science and Technology, Xinxiang Medical University, Jinsui Road 601, 453003 Xinxiang, China. e-mail: linjtlin@126.com and pangyufu@gmail.com

DOI: 10.14670/HH-18-017

Abbreviations. 4v, 4th ventricle; CA1, field Cornu Amonis 1 of the hippocampus; CA2, field Cornu Amonis 2 of the hippocampus; CA3, field Cornu Amonis 3 of the hippocampus; Cb, cerebellum; CNPase, 2',3'-Cyclic-nucleotide 3'-phosphodiesterase; CNS, central nerve system; cp, cerebral peduncle; CPu, caudate putamen; DG, dentate gyrus; DLG, dorsal lateral geniculate nucleus; DM, dorsomedial hypothalamic nucleus; ec, external capsule; fr, fasciculus retroflexus; Hi, hippocampus; icp, inferior cerebellar peduncle; GiA, gigantocellular nucleus; lc, locus coeruleus; LH, lateral hypothalamic area; LHb, lateral habenular nucleus; LP, lateral posterior thalamic nucleus; LSI, lateral septal nucleus, intermediate part; MAG, myelin-associated glycoprotein; MBP, myelin basic protein; Mfb, medial forebrain bundle; Myrf, myelin gene regulatory factor; mt, mammillothalamic tract; OLs, oligodendrocytes; OT, optic tract; PCRtA, parvicellular reticular nucleus alpha; PLP, myelin proteolipid protein; Po, posterior thalamic nuclear group; Sim, simple lobule; st, stria terminalis; VMH, ventromedial hypothalamic nucleus; VPM, ventral posteromedial thalamic nucleus; VP, ventral pallidum; ZI, zona incerta.

NPC1 mouse displays progressively neurological pathologies from postnatal day (P) 10 (Yan et al., 2014), e.g., axonal swelling, neuronal spheroids and presynaptic aggregates in the $Npc1^{-/-}$ cortex (Bu et al., 2002). Age-related neurodegeneration and gliosis have also been found in the brain and spinal cord as early as P10 (Pressey et al., 2012; Yan et al., 2014). Furthermore, inhibited myelination in $Npc1^{-/-}$ mice indicates that Npc1 protein is essential for maturation of oligodendrocytes (OLs) (Takikita et al., 2004; Yan et al., 2011).

In the CNS, OLs create myelin sheaths to surround the neuronal axon, providing critical metabolic supports for neuronal electrical signals (Hughes and Appel, 2016). The formation of myelin is precisely regulated by different factors and genes, e.g., myelin gene regulatory factor (Myrf), myelin basic protein (MBP), 2',3'-Cyclic-nucleotide 3'-phosphodiesterase (CNPase), myelin-associated glycoprotein (MAG) and myelin proteolipid protein (PLP). In $Npc1^{-/-}$ mice, pathological defects of myelination have been reported previously. For example, Myrf is an important transcription factor to promote myelination in the CNS (Emery et al., 2009). The expression of Myrf has been found to be decreased in the Npc1 mutant brain and spinal cord, resulting in a conspicuous hypomyelination (Yan et al., 2011). Furthermore, OL maturation in the $Npc1^{-/-}$ olfactory bulb is also defective, indicated by a decrease of CNPase and MBP at different stages, suggesting a general hypomyelination in $Npc1^{-/-}$ mice (Takikita et al., 2004; Yan et al., 2011).

Similar to NPC1 patients, Npc1 mutant mice show an age-related neuropathology in the different regions of the brain (Yan et al., 2014; Yu and Lieberman, 2013). However, detailed myelination impairment in the developing brain of $Npc1^{-/-}$ mice is still not fully understood. Therefore, in the present study, we performed immunohistochemistry to analyze myelination according to spatial- and temporal expression patterns of MBP in the mouse brain. Our results demonstrate that deficiency of Npc1 is sufficient to cause a severe and progressive perturbation of myelination in the brain.

Materials and methods

Animals

Heterozygous $Npc1^{+/-}$ mice (BALB/cNctr-*Npc1*$^{m1N/}$J) were purchased from the Jackson Laboratory (Bar Harbor, ME, USA) and used to generate $Npc1^{-/-}$ and wild type (WT) mice. Mice were maintained on a 12-hour light/dark cycle with *ad libitum* access to regular chow food and water. All experimental procedures were performed under the guidelines of the Ministry of Science and Technology of the People's Republic of China [(2006) 398] and approved by the Animal Care Committee of Xinxiang Medical University (No. 030032).

Genotype analysis

Genomic DNA extracted with phenol-chloroform from about 1 mm tail section of mice was used as a template for polymerase chain reaction (PCR) according to the protocol described previously (Loftus et al., 1997) using the primers suggested by the Jackson Laboratory.

Immunohistochemistry and image analysis

Mice were sacrificed and transcardially perfused with phosphate buffered saline (PBS) followed by 4% paraformaldehyde in 0.1 M PBS. Then, brains were post-fixed overnight in the same fixative. Frozen coronal sections (20 μm) were cut and collected using a cryostat (Leica CM1850, Wetzlar, Germany). Fluorescent immunostaining was performed according to the protocol described previously (Yan et al., 2014). Primary rat monoclonal antibody raised against MBP (1:300, Abcam, ab7349) and Cy3-labeled secondary antibody against rat IgG (1:500, Jackson Immuno Research) were used. Immunofluorescent images were acquired using a Nikon eclipse 80i fluorescence microscope (Shanghai, China). Digital images were adjusted in contrast and brightness with the Photoshop software (Adobe Systems, San Jose, CA).

Western blot analysis

Western blotting was performed as the protocol previously described (Yan et al., 2014). Briefly, tissues were collected and resuspended in homogenization buffer containing 5 mM HEPES, 0.5 mM EGTA, and 1x Complete Protease inhibitors (Roche Applied Science, Shanghai, China) at pH 7.4 and later homogenized. Protein concentrations were determined by a photometer (Tecan, Shanghai, China) using a Pierce bicinchoninic acid (BCA) protein assay kit (Beyotime, Shanghai, China). Equal amounts of protein (50 μg) from the samples were loaded on 10% sodium dodecyl sulfate (SDS)-polyacrylamide gels, followed by electrophoresis. The protein bands were then electro-transferred from gel into the nitrocellulose membrane (GE Healthcare, Beijing, China). The primary antibodies raised against MBP (1:1000, Abcam, Cambridge, MA) and glyceraldehyde-3-phosphate dehydrogenase (GAPDH; 1:10,000, Abcam) were used. The secondary antibodies with HRP-coupled goat anti-rat and mouse IgG (Santa Cruz, Heidelberg, Germany; 1:10,000) were used. The blots were developed with ECL Western blot substrate and exposed to Amersham Imager 600 blot imaging system (GE Healthcare, Beijing, China). Digital images were analyzed with Fiji/ImageJ.

RNA isolation and quantitative RT-PCR

Total RNA was extracted from the P35 cerebral cortex and hippocampus using Trizol reagent (Beyotime, Shanghai, China). The first cDNA was synthesized by

using 5X All-In-One RT MasterMix kit with dNTPs and random hexamer primers (abm, Richmond, Canada). These cDNAs served as the PCR template for PCR reactions using EvaGreen 2X qPCR MasterMix (abm) with a LightCycler® 96 Real-Time PCR System (Roche, Shanghai, China). GAPDH was used as an internal control for normalization. At least 3 replicates from four independent samples were performed. Primers used are as follows: PLP, 5'-GTGTTCTCCCATGGAATGCT-3' (forward) and 5'-TGAAGGTGAGCAGGGAAACT-3' (reverse); MAG, 5'-TGTGTAGCTGAGAAGGAGT ATGG-3' (forward) and 5'-ACAGTGCGATTCCAGAA GGATTAT-3' (reverse); MOG, 5'-GAGGGACAG AAGAACCCACA-3' (forward) and 5'-CAGTTCTC GACCCTTGCTTC-3' (reverse); CNPase, 5'-CCAAATTCTGTGACTACGGG-3' (forward) and 5'-GGTTTGCCC TTCCCATAGTA-3' (reverse); GAPDH, 5'-GACAGCCGCATCTTCTTGT-3' (forward) and 5'-CTTGCCGTGGGTAGAGTCAT-3' (reverse).

Statistical analysis

All data are expressed as mean ± SEM from at least three independent experiments. An unpaired Student's t-test was used for comparison between two groups and two-way repeated-measures ANOVA analysis was performed for three or more groups using GraphPad Prism Software Version 7. Post hoc analysis was performed using Bonferroni's multiple comparisons test. A p-value less than or equal to 0.05 was considered statistically significant.

Results

In the present study, results were arranged and presented by different regions of the brain and its developmental stages (Rao et al., 2011). The RT-PCR and Western blots showed that myelin genes and proteins were strongly decreased in different brain regions of the $Npc1^{-/-}$ mice (Fig. 1). To evaluate the precise differences among regions, MBP immunohistochemistry was performed in the forebrain including cerebral cortex, hippocampus and thalamus (Fig. 2); in the basal forebrain including septal nuclei, and anterior portion of the caudate-putamen (Fig. 3); in the midbrain including the middle to posterior portion of the midbrain (Fig. 4); in cerebellum (Fig. 5); and in the medulla oblongata of hindbrain (Fig. 6).

Decreases of myelin genes and proteins in $NPC1^{-/-}$ mice

To find alterations of myelination, we performed RT-PCR and Western blots to analyze expressions of different myelin genes and proteins in $Npc1^{-/-}$ mice. Our results showed that compared to WT mice, the amounts of mRNAs were strongly decreased at P35 in the cortex for PLP (27%±4.0), MAG (18%±1.7), MOG (33%±2.3) and CNPase (7%±0.09) (Fig. 1A) and in the hippocampus for PLP (25%±4.4), MAG (52%±7.9), MOG (61%±2.4) and CNPase (58%±1.7) (Fig. 1B). Furthermore, the Western blot analyses in different regions and stages demonstrated that the MBP expression in all investigated brain areas was strongly

Table 1. Summary of statistical analyses.

Figure	Sample size (n)	Statistical Test	Values
1A	Wild-type (n=4) $Npc1^{-/-}$ (n=4)	Two-tailed unpaired Student's t-test	PLP: t=17.69, P<0.0001 MAG: t=11.38, P<0.0001 MOG: t=16.38, P<0.0001 CNPase: t=12.36, P<0.0001
1B	Wild-type (n=4) $Npc1^{-/-}$ (n=4)	Two-tailed unpaired Student's t-test	PLP: t=13.34, P<0.0001 MAG: t=5.04, P=0.0031 MOG: t=4.038, P=0.0069 CNPase: t=18.76, P<0.0001
1D	Wild-type (n=3-4) $Npc1^{-/-}$ (n=3-4)	Two-way repeated-measure ANOVA Bonferroni's multiple comparisons test	Interaction: F=2.769, P=0.0608 Position: F=30.27, P<0.0001 Genotype: F=22.97, P=0.0003 Multiple comparison: Ob, P>0.9999; Cortex, P>0.9999; Hipp, P=0.0075; Cb, P=0.016; Mb, P=0.2201; Hb, P>0.9999
1E	Wild-type (n=3-4) $Npc1^{-/-}$ (n=3-4)	Two-way repeated-measure ANOVA Bonferroni's multiple comparisons test	Interaction: F=3.228, P=0.0355 Position: F=37.66, P<0.0001 Genotype: F=83.38, P<0.0001 Multiple comparison: Ob, P=0.0125; Cortex, P=0.0012; Hipp, P=0.0003; Cb, P=0.7153; Mb, P=0.008; Hb, P=0.3373
1F	Wild-type (n=5) $Npc1^{-/-}$ (n=5)	Two-way repeated-measure ANOVA Bonferroni's multiple comparisons test	Interaction: F=3.358, P=0.0186 Position: F=1.315, P=0.2896 Genotype: F=131, P<0.0001 Multiple comparison: Ob, P<0.0001; Cortex, P<0.0001; Hipp, P<0.0001; Cb, P=0.0006; Mb, P=0.0146; Hb, P=0.5204

decreased at P35 in the Npc1$^{-/-}$ mouse (Fig. 1C-F and Table 1) besides a small change in the hindbrain (Hb in Fig. 1C-F and Table 1). At P9, the expression was only reduced in the hippocampus (Hipp), the cerebellum (Cb) and the midbrain (Mb) (Fig. 1C-D). Taken together, these data strongly suggest perturbed myelination in Npc1$^{-/-}$ mice.

MBP expression in the forebrain

In the Npc1$^{-/-}$ forebrain at P9, MBP protein expression was not observed in the caudate putamen (CPu); however, it was expressed very weakly in the external capsule (ec), the stria terminalis (st), and partially expressed in the locus coeruleus (lc). The MBP expression seemed to be normal in ventral posteromedial thalamic nucleus (VPM) (Fig. 2F-H) when compared to the same stage in WT mice (Fig. 2B-D). At P35 and P60, MBP expression was strong throughout the whole brain (Fig. 2J-L,R-T) in WT mice, but dramatically decreased in the cortex and the posterior thalamic nuclei (Po) of the thalamus (Fig. 2N-P,V-X), and even disappeared in the hippocampus (Fig. 2P,X) in the Npc1$^{-/-}$ mice. Furthermore, in the Npc1$^{-/-}$ basal forebrain region, MBP

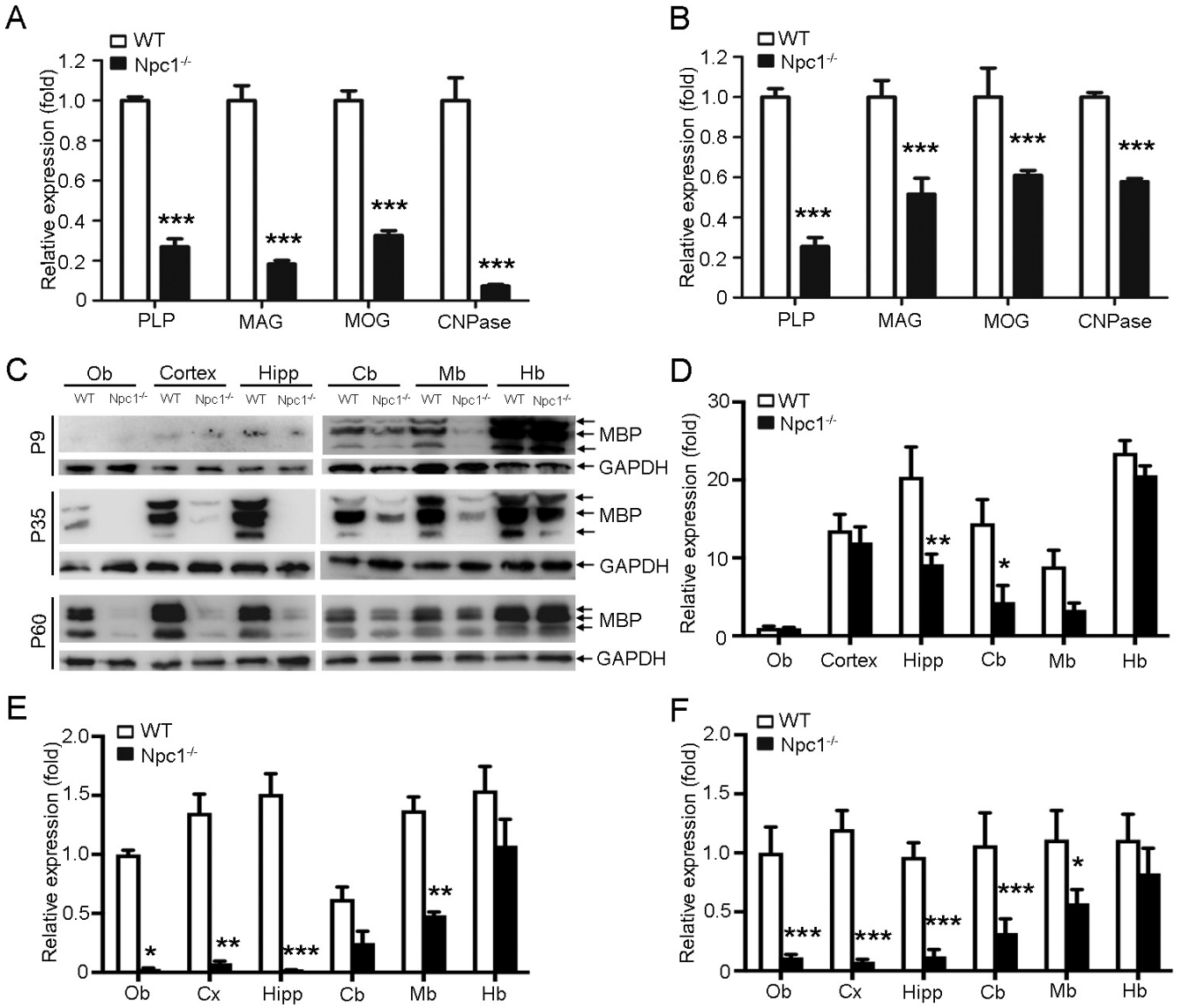

Fig. 1. Myelin genes and protein analysis in the NPC1$^{-/-}$ mice. **A, B.** Quantitative analysis of PLP, MAG, MOG and CNPase mRNAs by real-time RT-PCR in the NPC1$^{-/-}$ hippocampus; all data are normalized to the control (the wild type, indicated as 1). **C-F.** Western blot and semi-quantitative analysis for MBP protein in the different parts of brain at P9, P35 and P60; the expression level of olfactory bulb (Ob) in the WT mice as control for each stage. All data are presented as mean±SEM from at least 3 independent experiments (* $p<0.05$, ** $p<0.01$, and *** $p<0.001$).

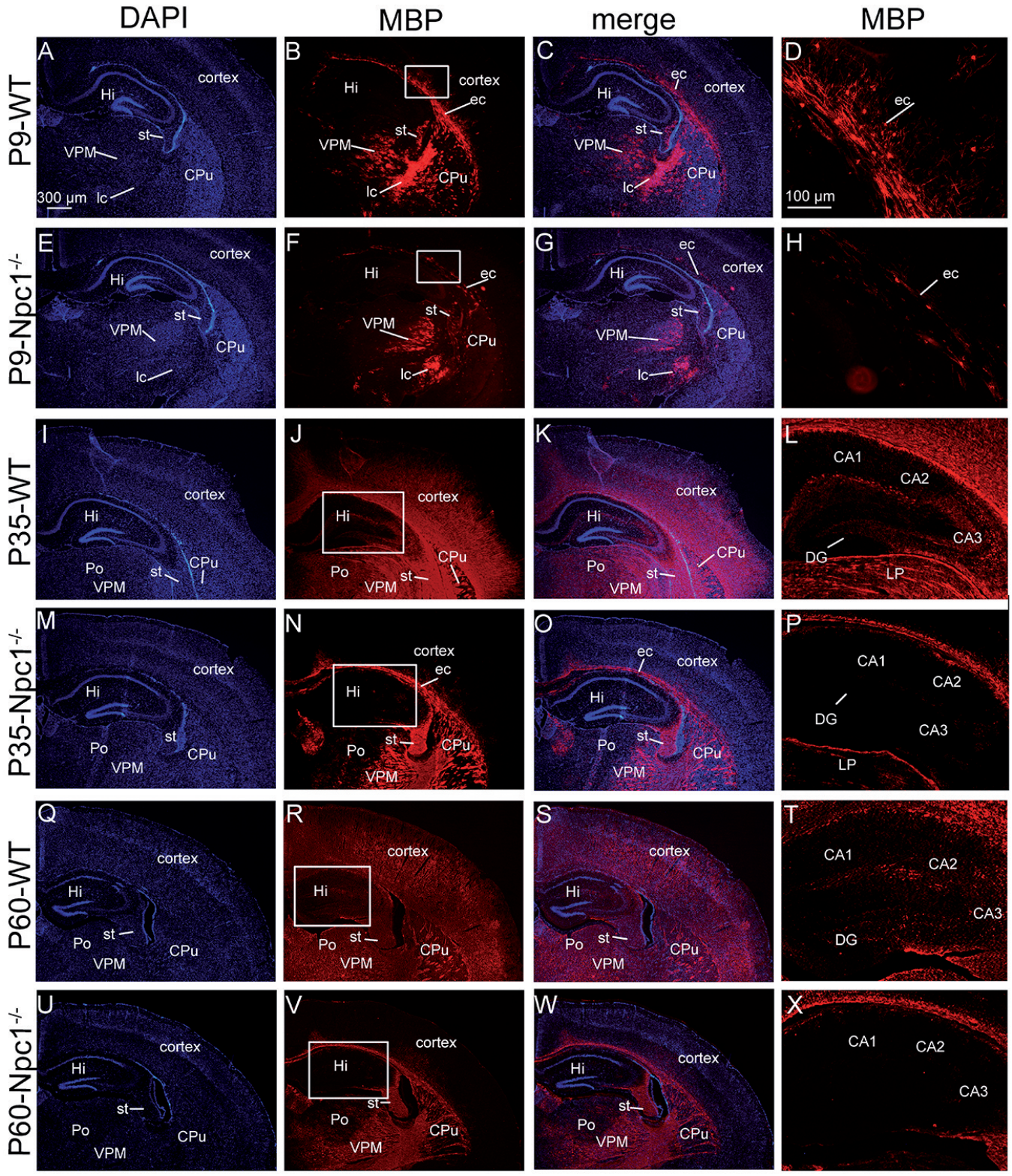

Fig. 2. Decreased MBP expression in the NPC1$^{-/-}$ forebrain. **A-H.** Photomicrographs demonstrate the decreased MBP immunoreactivity at P9. **D, H** demonstrate the magnification of the boxed areas in (**B, F**), respectively. **I-P.** Photomicrographs demonstrate the decreased MBP immunoreactivity at P35. **L, P** demonstrate the magnification of the boxed areas in (**J, N**), respectively. **Q-X.** Photomicrographs demonstrate the decreased MBP immunoreactivity at P60. **T, X** demonstrate the magnification of the boxed areas in (**R, V**), respectively. Scale bars: D, H, L, P, T, X, 100 μm; A-C, E-G, I-K, M-O, Q-S, U-W, 300 μm.

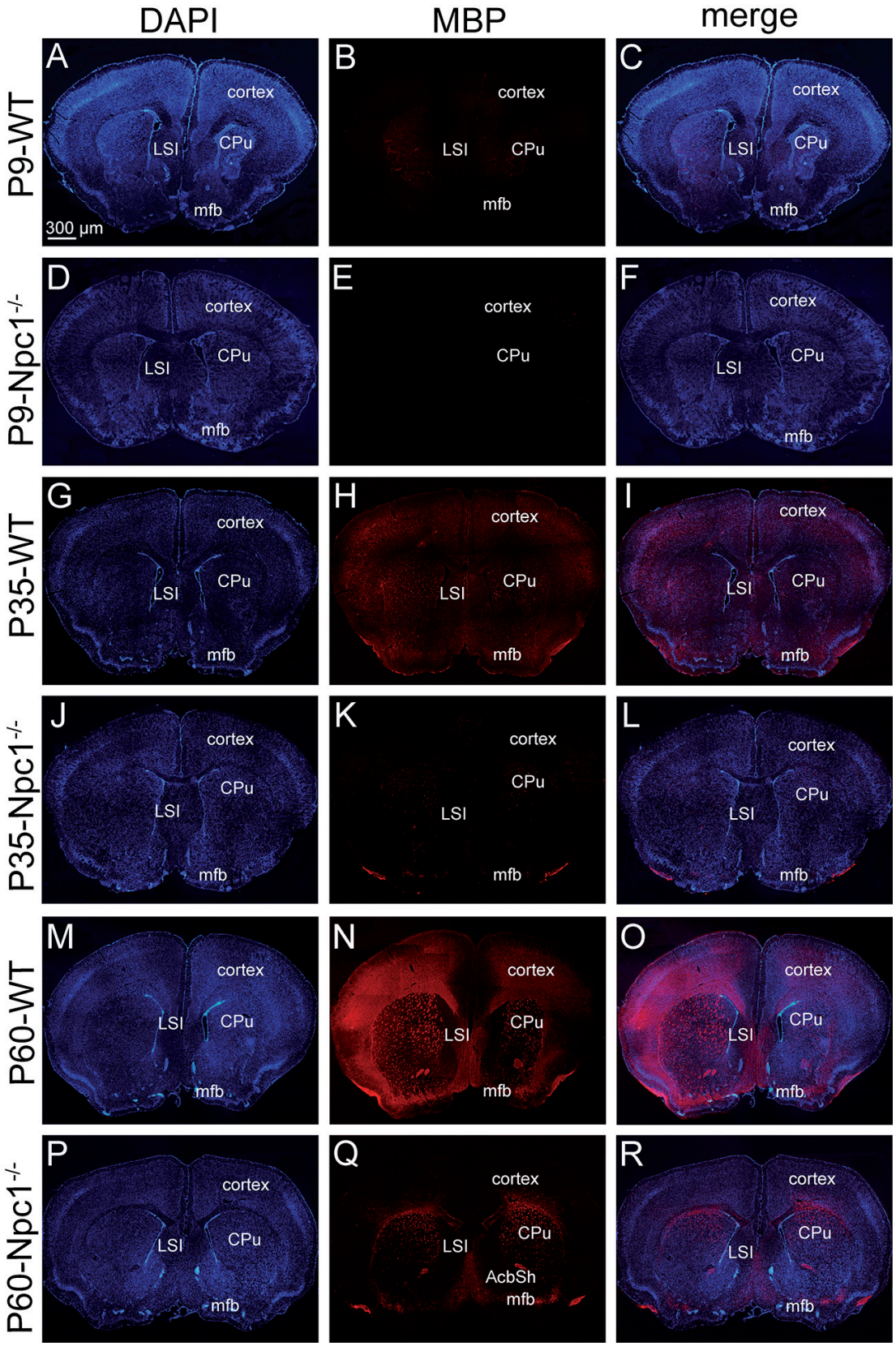

Fig. 3. Abnormal expression of MBP in the basal forebrain of the NPC1$^{-/-}$ mouse at P9 **(A-F)**, P35 **(G-L)** and P60 **(M-R)** detected by immunohistochemistry. Scale bar: 300 μm.

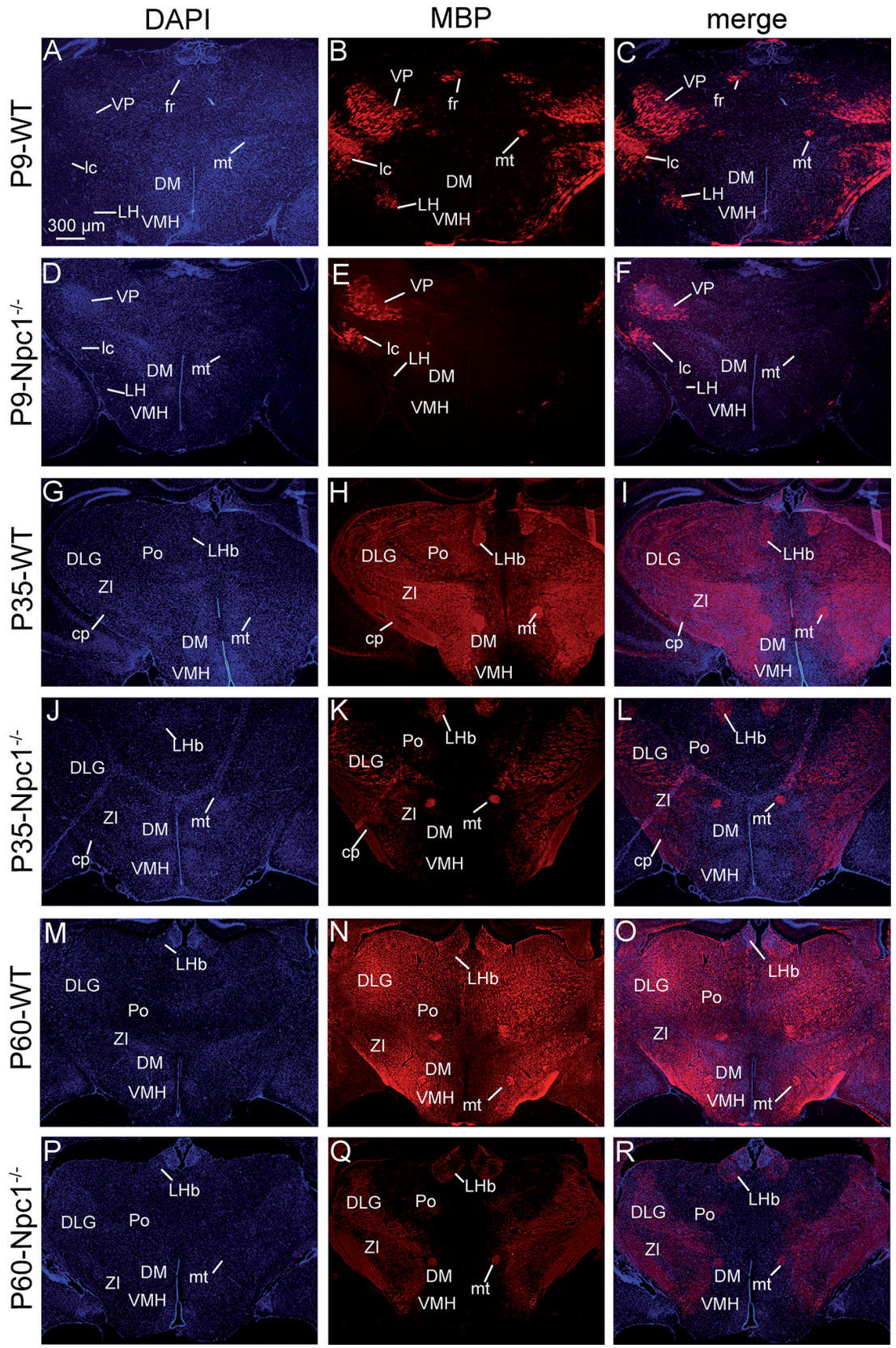

Fig. 4. Abnormal expression of MBP in the thalamus and hypothalamus of the NPC1$^{-/-}$ mouse at P9 **(A-F)**, P35 **(G-L)** and P60 **(M-R)** detected by immunohistochemistry. **A-F**, At P9, the expression of MBP is found in the fr, mt, LH, VMH in WT mice, but not in the NPC1$^{-/-}$ mice; At P35 **(G-L)** and P60 **(M-R)**, MBP is strongly decreased in the middle region of thalamus and in the hypothalamus of the NPC1$^{-/-}$ mice. Scale bar: 300 μm.

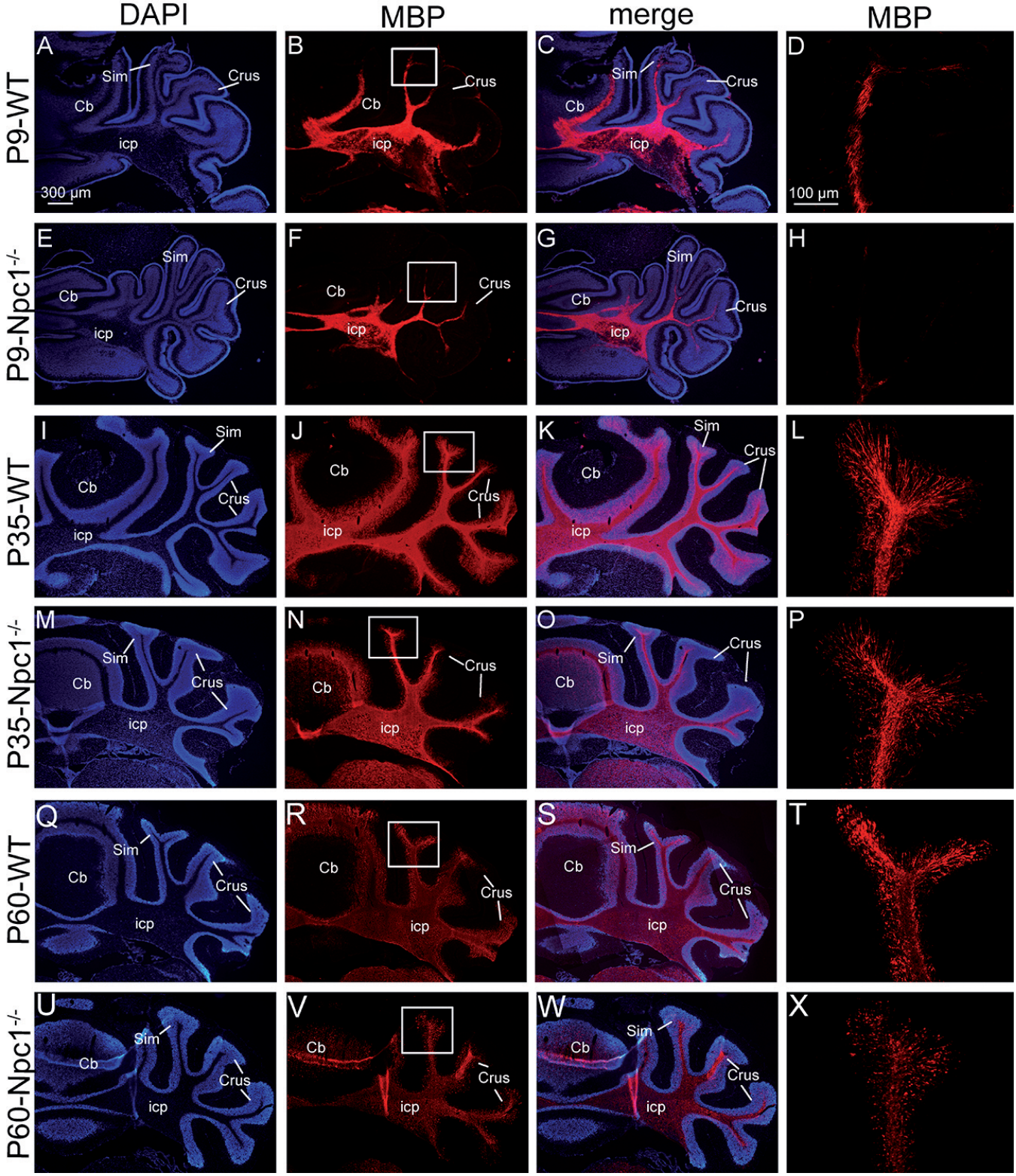

Fig. 5. Defected MBP expression in the NPC1$^{-/-}$ cerebellum at P9 **(A-H)**, P35 **(I-P)** and P60 **(Q-X)** detected by immunohistochemistry. D, H, L, P, T and X show the magnifications of the boxes in B, F, J, N, R and V respectively. Scale bars: D, H, L, P, T, X; 100 μm; A-C, E-G, I-K, M-O, Q-S, U-W, 300 μm.

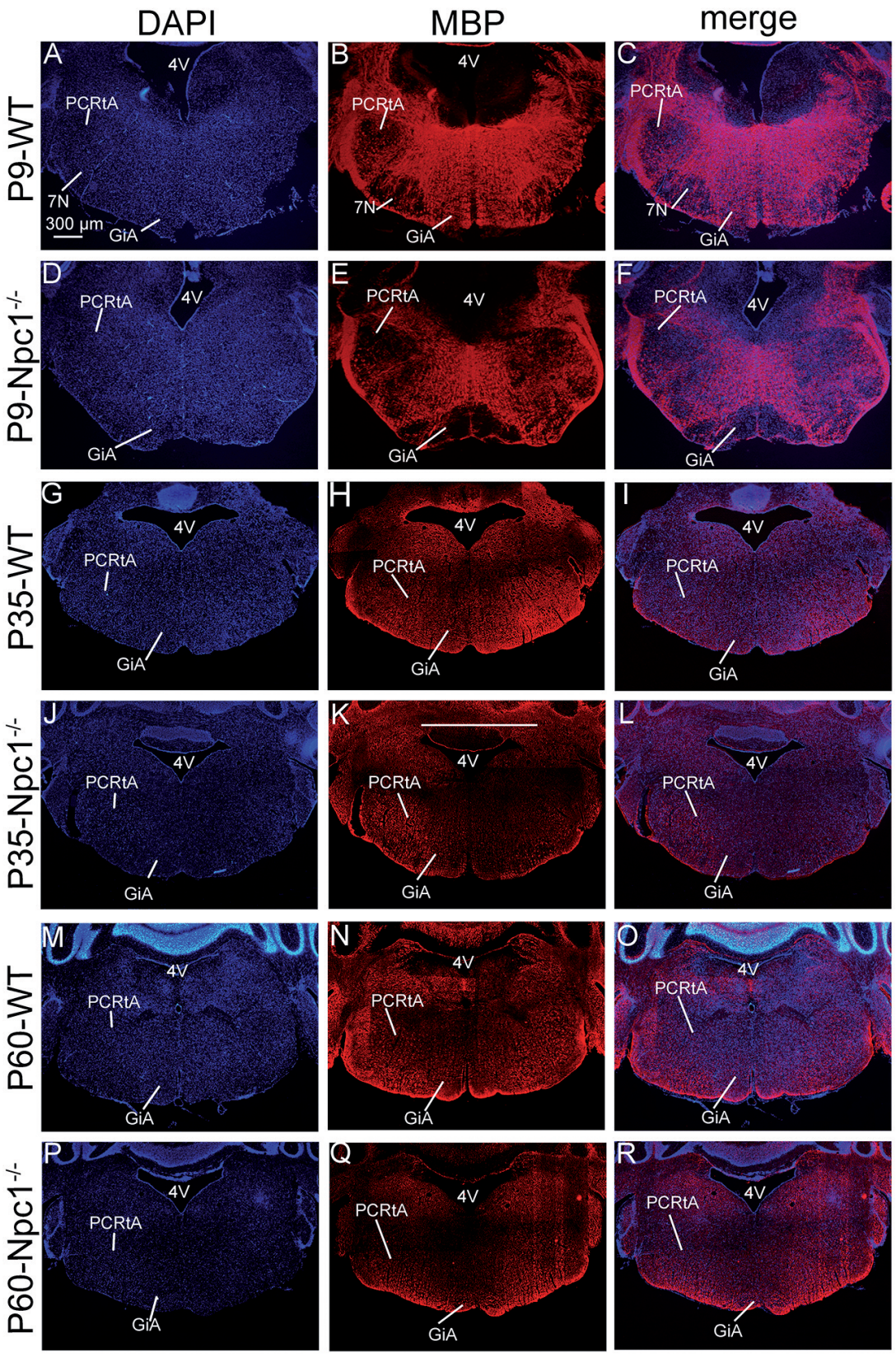

Fig. 6. Abnormal expression of MBP in the hindbrain of the NPC1$^{-/-}$ mouse at P9 **(A-F)**, P35 **(G-L)** and P60 (**M-R**) detected by immunohistochemistry. Scale bar: 300 μm.

expression was strongly decreased in the cortex and the CPu, especially at later stages (Fig. 3). Altogether, these results reveal a dynamic and pronounced reduction of myelin proteins in the Npc1$^{-/-}$ forebrain, especially in the cortex and hippocampus (Fig. 2).

MBP expression in the thalamus and hypothalamus

In the midbrain, MBP signals were prominent in the ventral pallidum (VP), lc, lateral hypothalamic area (LH), mammillothalamic tract (mt), and optic tract (OT) at P9 in WT mice (Fig. 4A-C). However, signals found in VP and lc regions in Npc1$^{-/-}$ midbrain had a strongly reduced intensity (Fig. 4 D-F). At P35, MBP labeling was observed in most regions of WT midbrain with a high level in zona incerta (ZI) and other regions (Fig. 4H,I). At P65, MBP labeling increased strongly and was observed in all regions of WT midbrain (Fig. 4N,O). In contrast, in the Npc1$^{-/-}$ mice, MBP expression was strongly reduced (Fig. 4K,Q), especially in the ventral media areas of the thalamus and hypothalamus where the signals were almost absent. Western blot analyses also identified a significant decrease of MBP in the midbrain of Npc1$^{-/-}$ mice from P9 onwards in the Npc1$^{-/-}$ mice (Fig. 1).

MBP expression in the cerebellum

In the WT cerebellum, MBP expression was strong in the white matter of the inferior cerebellar peduncle (icp) (Fig. 5B,N,R) and of lobules (Fig. 5B,N,R), but not in the granule cell layer at P9. At P35, myelin structures were found in the granule cell layer with a moderate intensity (Fig. 5L,T). In Npc1$^{-/-}$ mice, the expression of MBP protein was apparently normal in the icp, but its expression in the cerebellar lobules was reduced, especially in the granule cell layer (Fig. 5H,P,X). The Western blot analyses also identified a decrease of MBP in the cerebellum of Npc1$^{-/-}$ mice from P9 onwards (Fig. 1).

MBP expression in the hindbrain

In WT mice, MBP signals were found to be broad in all areas of the hindbrain (Fig. 6). However, at P9 in Npc1$^{-/-}$ mice, signals were weaker compared to WT mice, especially in the parvicellular reticular nucleus alpha (PCRtA) and gigantocellular nucleus (GiA) regions (Fig. 6). From P35, the expression patterns of MBP in both WT and Npc1$^{-/-}$ mice were similar (Figs. 1, 6).

Discussion

NPC1 disease is a progressive neurological disorder characterized by a widespread gliosis, dysmyelination and neurodegeneration (Ong et al., 2001; Takikita et al., 2004; Yan et al., 2014). The Npc1$^{-/-}$ mouse mimics clinical symptoms of the human NPC1 neuropathology (Boothe et al., 1984), including cerebral atrophy, dysmyelination and neuronal degeneration, as well as cognitive impairment for learning and memory (German et al., 2002; Võikar et al., 2002; Baudry et al., 2003; Sarna et al., 2003). Therefore, it is a useful mouse model to study potential mechanisms and therapeutics of the NPC1 disease.

Pathological changes of myelination have been well investigated in both NPC1 patients and Npc1 mutant mice. In NPC1 patients, MRI scanning shows a strong reduction of gray matter volume in the insular cortex, hippocampus, thalamus and cerebellum, but a lesser reduction in the striatum (Walterfang et al., 2010). Similar to NPC1 patients, myelination was also disrupted in the brain of Npc1$^{-/-}$ mice. For example, MRI imaging showed diminished myelination in the Npc1$^{-/-}$ corpus callosum, putamen and thalamus (Ahmad et al., 2005; Totenhagen et al., 2012). In the present study, myelination was found to be decreased strongly in the olfactory bulb, cortex, hippocampus, thalamus and hypothalamus of Npc1$^{-/-}$ mice, moderately in the cerebellum, and slightly in the hindbrain. Compared to MRI data, our results suggest a more widespread reduced myelination in the Npc1 mutant brain. Therefore, the present study extends those previous findings and further demonstrates altered myelination in detail in different brain regions during the development of Npc1$^{-/-}$ mice.

The differentiation and maturation of OLs involves several distinct stages that can be regulated by different factors (van Tilborg et al., 2018). In the final stage, the maturation of OLs is associated with up-regulation of myelin genes and proteins, e.g., Myrf, PLP, CNPase and MBP (Emery et al., 2009). Myrf is a crucial transcription factor for the regulation of most myelin genes and is regulated by Npc1 protein (Emery et al., 2009; Yan et al., 2011). The present data indicate that myelination is less affected in the hindbrain than in the forebrain form P35 in the Npc1$^{-/-}$ mice (Fig. 1). Interestingly, the previous study showed that, in the hindbrain, Myrf is expressed early at P3 and most of the OLs differentiate into mature form in the Npc1$^{-/-}$mice. However, in the forebrain, Myrf is expressed late over the first 2 weeks postnatal and myelination is strongly affected by *Npc1* deletion (Figs. 1-3; Emery et al., 2009). These findings suggest that Npc1 protein may regulate myelination via the spatiotemporal regulation of Myrf gene (Yan et al., 2011).

In the developing mouse brain, the formation of myelin is also a highly dynamic process regulated by neuron-glial interaction. For example, conditional deletion of *Npc1* gene in neurons leads to the defect of OL maturation, which is associated with loss of myelination signals from axons to OLs, while deletion of *Npc1* in OLs alone only causes delayed myelination from early postnatal days (Yu and Lieberman, 2013). Furthermore, astrocytes have a major role in the synthesis and transportation of cholesterol to neurons (Wasser et al., 2007). Using genetic modification to overexpress wild type *Npc1* gene in astrocytes leads to

enhanced survival and restored myelin tracts in the Npc1$^{-/-}$ mice (Zhang et al., 2008). These findings suggest that Npc1 might be a key regulator in the neuron-glial interaction. Therefore, further study should be continued to investigate precisely how Npc1 regulates the neuron-oligodendroglial communication and maturation of CNS myelin.

Acknowledgements: The authors would like to thank Christopher Bishop for his critical correction of this manuscript. This work is supported by the National Natural Science Foundation of China (81400936, U1304808, 81600987, 81771226), Xinxiang City Foundation (CXRC16003 and ZD17008) and Xinxiang Medical University Foundation (20172DCG-03).

Conflict of interest. The authors declare no competing financial interests.

Author's contributions. JL and XY conceived this study. LQ, EY, JKL and XY designed and performed the experiments. JKL, JL and XY wrote the manuscript.

References

Ahmad I., Lope-Piedrafita S., Bi X., Hicks C., Yao Y., Yu C., Chaitkin E., Howison C.M., Weberg L., Trouard T.P. and Erickson R.P. (2005). Allopregnanolone treatment, both as a single injection or repetitively, delays demyelination and enhances survival of Niemann-Pick C mice. J. Neurosci. Res. 82, 811-821.

Baudry M., Yao Y., Simmons D., Liu J. and Bi X. (2003). Postnatal development of inflammation in a murine model of Niemann-Pick type C disease: immunohistochemical observations of microglia and astroglia. Exp. Neurol. 184, 887-903.

Boothe A.D., Weintroub H., Pentchev P.G., Jones J., Butler J., Barry J.E., Neumeyer B., Stivers J.A. and Brady R.O. (1984). A lysosomal storage disorder in the BALB/c mouse: bone marrow transplantation. Vet. Pathol. 21, 432-441.

Bu B., Li J., Davies P. and Vincent I. (2002). Deregulation of cdk5, hyperphosphorylation, and cytoskeletal pathology in the Niemann-Pick type C murine model. J. Neurosci. 22, 6515-6525.

Emery B., Agalliu D., Cahoy J.D., Watkins T.A., Dugas J.C., Mulinyawe S.B., Ibrahim A., Ligon K.L., Rowitch D.H. and Barres B.A. (2009). Myelin gene regulatory factor is a critical transcriptional regulator required for CNS myelination. Cell 138, 172-185.

German D.C., Liang C.L., Song T., Yazdani U., Xie C. and Dietschy J.M. (2002). Neurodegeneration in the Niemann-Pick C mouse: glial involvement. Neuroscience 109, 437-450.

Hughes E.G. and Appel B. (2016). The cell biology of CNS myelination. Curr. Opin. Neurobiol. 39, 93-100.

Loftus S.K., Morris J.A., Carstea E.D., Gu J.Z., Cummings C., Brown A., Ellison J., Ohno K., Rosenfeld M.A., Tagle D.A., Pentchev P.G. and Pavan W.J. (1997). Murine model of Niemann-Pick C disease: mutation in a cholesterol homeostasis gene. Science 277, 232-235.

Ong W.Y., Kumar U., Switzer R.C., Sidhu A., Suresh G., Hu C.Y. and Patel S.C. (2001). Neurodegeneration in Niemann-Pick type C disease mice. Exp. Brain Res. 141, 218-231.

Pressey S.N.R., Smith D.A., Wong A.M.S., Platt F.M. and Cooper J.D. (2012). Early glial activation, synaptic changes and axonal pathology in the thalamocortical system of Niemann-Pick type C1 mice. Neurobiol. Dis. 45, 1086-1100.

Rao D.B., Little P.B., Malarkey D.E., Herbert R.A. and Sills R.C. (2011). Histopathological evaluation of the nervous system in National Toxicology Program rodent studies: a modified approach. Toxicol. Pathol. 39, 463-470.

Sarna J.R., Larouche M., Marzban H., Sillitoe R.V., Rancourt D.E. and Hawkes R. (2003). Patterned Purkinje cell degeneration in mouse models of Niemann-Pick type C disease. J. Comp. Neurol. 456, 279-291.

Subramanian K. and Balch W.E. (2008). NPC1/NPC2 function as a tag team duo to mobilize cholesterol. Proc. Natl. Acad. Sci. USA 105, 15223-15224.

Takikita S., Fukuda T., Mohri I., Yagi T. and Suzuki K. (2004). Perturbed myelination process of premyelinating oligodendrocyte in Niemann-Pick type C mouse. J. Neuropathol. Exp. Neurol. 63, 660-673.

Totenhagen J.W., Lope-Piedrafita S., Borbon I.A., Yoshimaru E.S., Erickson R.P. and Trouard T.P. (2012). In vivo assessment of neurodegeneration in Niemann-Pick type C mice by quantitative T2 mapping and diffusion tensor imaging. J. Magn. Reson. Imaging 35, 528-536.

van Tilborg E., de Theije C.G.M., van Hal M., Wagenaar N., de Vries L.S., Benders M.J., Rowitch D.H. and Nijboer, C.H. (2018). Origin and dynamics of oligodendrocytes in the developing brain: Implications for perinatal white matter injury. Glia 66, 221-238.

Võikar V., Rauvala H. and Ikonen E. (2002). Cognitive deficit and development of motor impairment in a mouse model of Niemann-Pick type C disease. Behav. Brain Res. 132, 1-10.

Walterfang M., Fahey M., Desmond P., Wood A., Seal M.L., Steward C., Adamson C., Kokkinos C., Fietz M. and Velakoulis D. (2010). White and gray matter alterations in adults with Niemann-Pick disease type C: a cross-sectional study. Neurology 75, 49-56.

Wasser C.R., Ertunc M., Liu X. and Kavalali E.T. (2007). Cholesterol-dependent balance between evoked and spontaneous synaptic vesicle recycling. J. Physiol. 579, 413-429.

Yan X., Lukas J., Witt M., Wree A., Hübner R., Frech M., Köhling R., Rolfs A. and Luo J. (2011). Decreased expression of myelin gene regulatory factor in Niemann-Pick type C 1 mouse. Metab. Brain Dis. 26, 299-306.

Yan X., Yang F., Lukas J., Witt M., Wree A., Rolfs A. and Luo J. (2014). Hyperactive glial cells contribute to axonal pathologies in the spinal cord of Npc1 mutant mice. Glia 62, 1024-1040.

Yu T. and Lieberman A.P. (2013). Npc1 acting in neurons and glia is essential for the formation and maintenance of CNS myelin. PLoS Genet. 9, e1003462.

Zhang M., Strnatka D., Donohue C., Hallows J.L., Vincent I. and Erickson R.P. (2008). Astrocyte-only Npc1 reduces neuronal cholesterol and triples life span of Npc1$^{-/-}$ mice. J. Neurosci. Res. 86, 2848-2856.

Accepted June 29, 2018